2 μm solid-state laser mode-locked by single-layer graphene

A. A. Lagatsky,[1] Z. Sun,[2] T. S. Kulmala,[2] R. S. Sundaram,[2] S. Milana,[2] F. Torrisi,[2] O. L. Antipov,[3] Y. Lee,[4] J. H. Ahn,[4] C. T. A. Brown,[1] W. Sibbett,[1] and A. C. Ferrari[2,a)]
[1]*School of Physics and Astronomy, University of St Andrews, St Andrews KY16 9SS, United Kingdom*
[2]*Department of Engineering, University of Cambridge, Cambridge CB3 0FA, United Kingdom*
[3]*Institute of Applied Physics, Russian Academy of Sciences, Nizhny Novgorod, Russia*
[4]*School of Advanced Materials Science and Engineering and Advanced Institute of Nanotechnology, Sungkyunkwan University, Suwon 440-746, Korea*

(Received 25 October 2012; accepted 17 December 2012; published online 10 January 2013)

We report a 2 μm ultrafast solid-state $Tm:Lu_2O_3$ laser, mode-locked by single-layer graphene, generating transform-limited ~410 fs pulses, with a spectral width ~11.1 nm at 2067 nm. The maximum average output power is 270 mW, at a pulse repetition frequency of 110 MHz. This is a convenient high-power transform-limited ultrafast laser at 2 μm for various applications, such as laser surgery and material processing. © *2013 American Institute of Physics*. [http://dx.doi.org/10.1063/1.4773990]

Ultrafast lasers operating at ~2 μm are of great interest due to their potential in various applications, e.g., telecoms, medicine, material processing, and environment monitoring.[1–5] They can be used for light detection and ranging measurements and free-space optical communications, due to the 2–2.5 μm atmospheric transparency window.[5] Because water (main constituent of human tissue) absorbs more at ~2 μm (~100/cm) (Ref. 3) than at other conventional laser wavelengths (e.g., ~10/cm at ~1.5 μm, and ~1/cm at ~1 μm),[3] sources working at ~2 μm are promising for medical diagnostics[3] and laser surgery.[3] Currently, the dominant approach to ultrafast pulse generation at 2 μm relies on semiconductor saturable absorber mirrors (SESAMs).[6,7] InGaAsSb quantum-well-based SESAMs were used to mode-lock $Tm,Ho:NaY(WO_4)_2$ (Ref. 8) and $Tm:Sc_2O_3$ (Ref. 9) lasers, generating 258 fs pulses with 155 mW output power at 2 μm[8] and 246 fs pulses with 325 mW output at 2.1 μm.[9] However, SESAMs require complex growth techniques (e.g., molecular beam epitaxy[6]), often combined with ion implantation[8,9] to reduce recovery time.[6,7]

Nanotubes and graphene have emerged as promising saturable absorbers (SAs), due to their low saturation intensity,[10–14] low-cost,[10] and easy fabrication.[12,14,15] With nanotubes, broadband operation can be achieved by using a distribution of tube diameters.[10,16] With graphene, this is intrinsic, due to the gapless linear dispersion of Dirac electrons.[12,14] Ultrafast pulse generation at 0.8,[17] 1,[18] 1.3,[19] and 1.5 μm (Refs. 10–12, 14, 20–23) was demonstrated with graphene-based SAs (GSAs). Zhang *et al.*[25] reported a 1.94 μm Tm-doped fiber laser mode-locked by a polymer composite with graphene produced by liquid phase exfoliation of graphite.[14,24] Compared to solid-state lasers, fiber lasers have some advantages, such as compact geometry and alignment-free operation. However, their output power is typically very low (~mW (Ref. 26)) and their output spectrum generally has side-bands.[26] Solid-state lasers have the advantage, compared to fibre lasers, of sustaining ultrafast pulses with higher output power (typically $\geq$ 100 mW) (Refs. 6 and 7) and better pulse quality (e.g., transform-limited with sideband-free profile in the spectral domain[6,7]). Therefore, solid-state lasers are of interest for applications requiring high power and good pulse quality, such as industrial material processing[6] and laser surgery.[3] Liu *et al.*[27] used graphene-oxide to mode-lock a 2 μm solid-state $Tm:YAlO_3$ laser. However, the output pulse duration was long, ~10 ps, due to the lack of intracavity dispersion compensation.[27] Also, graphene oxide is fundamentally different from graphene: it is insulating with a mixture of sp^2/sp^3 regions[29,30] and with many defects and gap states.[30] Thus it may not offer the same wideband tunability as graphene. A mixture of 1 or 2 graphene layers grown by chemical vapor deposition (CVD) was used to mode-lock a Tm-doped calcium lithium niobium gallium garnet (Tm:CLNGG) laser at 2 μm in Ref. 28. However, compared to 2 μm solid-state lasers mode-locked by SESAMs,[8,9] the output power was low (~60 mW), limited by damage to the mode-locker.

Here we report a single-layer graphene (SLG) mode-locked solid-state $Tm:Lu_2O_3$ laser at ~2067 nm, with a 270 mW average output power. Transform-limited ~410 fs pulses are generated using a dispersion-compensated cavity. This is a convenient high-power transform-limited laser at 2 μm for various applications.

Our GSA is prepared as follows. SLG is grown by CVD.[31,32] A ~35 μm thick Cu foil is heated to 1000 °C in a quartz tube, with 10 sccm H_2 flow at $\sim 5 \times 10^{-2}$ Torr. The H_2 flow is maintained for 30 min. This not only reduces the oxidized foil surface, but also extends the graphene grain size. The precursor gas, a $H_2:CH_4$ mixture with flow ratio 10:15, is injected at a pressure of 4.5×10^{-1} Torr for 30 min. The carbon atoms are then adsorbed onto the Cu surface and nucleate SLG via grain propagation.[31,32] The quality and number of layers are investigated by Raman spectroscopy,[33,34] Fig. 1. At the more common 514 nm excitation, the Raman spectrum of CVD graphene on Cu does not show a flat background, due to Cu photoluminescence.[35] This can be suppressed at 457 nm, Fig. 1. The spectrum does not show a D peak, indicating negligible defects.[33,34,36] The 2D peak is a single sharp Lorentzian, signature of SLG.[33]

a)Electronic mail: acf26@eng.cam.ac.uk.

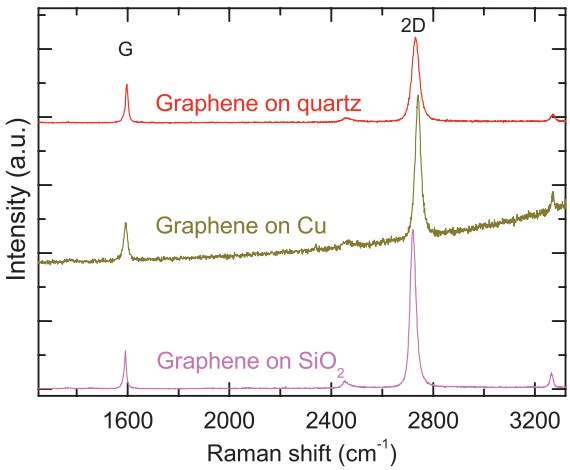

FIG. 1. Raman spectra at 457 nm for graphene on Cu (before transfer) and after transfer on quartz and SiO_2/Si.

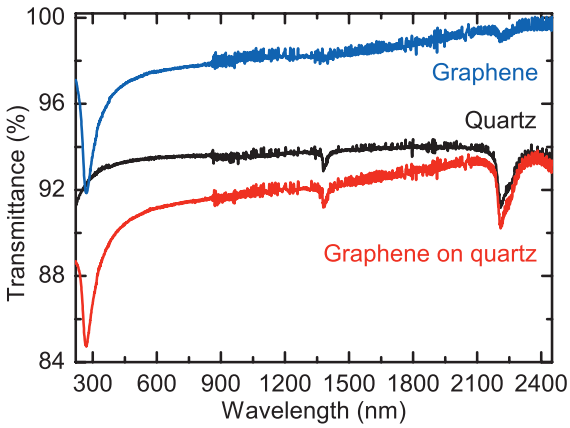

FIG. 2. Transmittance of quartz and graphene on quartz. For graphene, this is derived from the transmittance of transferred graphene on quartz divided by that of quartz.

We then transfer a $10 \times 10\,mm^2$ SLG region onto a quartz substrate (3 mm thick) as follows. Poly(methyl methacrylate) (PMMA) is spin-coated on the sample. Cu is then dissolved in a 3% H_2O_2 : 35% HCl (3:1 ratio) mixture, further diluted in equal volume of deionized water. The PMMA/graphene/Cu foil is then left floating until all Cu is dissolved. The remaining PMMA/graphene film is cleaned by moving it to a deionized H_2O bath, a 0.5 M HCl bath, and again to a deionized H_2O bath. Finally, the layer is picked up using the target quartz substrate and left to dry under ambient conditions. After drying, the sample is heated to 180 °C for 20 min to flatten out any wrinkles.[37] The PMMA is then dissolved in acetone, leaving SLG on quartz. This is then inspected by optical microscopy, Raman spectroscopy, and absorption microscopy. A representative Raman spectrum of the transferred sample is in Fig. 1. After transfer, the 2D peak is still a single sharp Lorentzian, validating that SLG has indeed been transferred. The absence of a D peak proves that no structural defects are induced during this process.[33,34,36,38] In order to estimate the doping, an analysis of more than 15 measurements with 514 nm excitation is carried out. This wavelength is used since most previous literature and correlations were derived at 514 nm.[39] We find that the G peak position, Pos(G), up-shifts $\sim 4\,cm^{-1}$ in average after transfer on quartz, whereas the full width at half maximum of the G peak, FWHM(G), decreases from ~17 to $\sim 10.5\,cm^{-1}$. Also, the 2D to G intensity and area ratios, I(2D)/I(G); A(2D)/A(G), decrease from 3.2 to 1.6 and 5.8 to 5.3, respectively. This implies an increased p-doping compared to graphene on Cu before transfer.[39–41] We estimate the doping for the sample on quartz to be $\sim 10^{13}\,cm^{-2}$, corresponding to a Fermi level shift ~300/400 meV. For comparison, we also transferred on SiO_2/Si. In this case, the average Pos(G) and FWHM(G) are $1584\,cm^{-1}$ and $14\,cm^{-1}$. The average Pos(2D) is $2685\,cm^{-1}$, and I(2D)/I(G); A(2D)/A(G) are 3.2 and 7.1. This indicates a much lower doping, below 100 meV. Therefore, we conclude that the doping of our graphene transferred on quartz does not arise from the transfer process itself, but it is most likely due to charge transfer from adsorbates on the substrate.[42,43] The transmittance of the transferred SLG on quartz is then measured (Fig. 2). The band at ~270 nm is a signature of the van Hove singularity in the graphene density of states,[44] while those at ~1.4, 2.2 μm are due to quartz.[45] The transmittance in the visible range (e.g., at ~700 nm) is ~97.7% (i.e., ~2.3% absorbance), further confirming that the sample is indeed SLG.[46] The absorbance decreases to ~1% at 2067 nm, much lower than the 2.3% expected for intrinsic SLG. We assign this to doping.[47] The graphene optical conductivity σ at a wavelength λ is $\sigma(\lambda, E_F, T) = \frac{\pi e^2}{4h}\left[\tanh\left(\frac{\frac{hc}{\lambda}+2E_F}{4k_BT}\right)+\tanh\left(\frac{\frac{hc}{\lambda}-2E_F}{4k_BT}\right)\right]$, as for Ref. 47, where T is the temperature, E_F the Fermi energy. The transmittance (Tr) is linked to σ as[47] $Tr \approx 1 - \frac{4\pi\sigma}{c}$. By fitting to the measured Tr, we derive $E_F \sim 350$ meV, consistent with the Raman estimates.

The laser setup is shown in Fig. 3. The cavity consists of four plano-concave high-reflectivity (R > 99.2% at 2 μm) mirrors (M1–M4) and an output coupler (OC) with 1% transmittance at 2 μm, and is designed to ensure the best mode-matching between the pump and intra-cavity laser beams. Tm : Lu_2O_3 ceramic is selected as the gain material because of its high thermal conductivity,[48] broad emission spectrum (>1.9 – 2.1 μm (Refs. 48 and 49)), high absorption,[48,49] and emission cross-sections,[48,49] making it suitable for high-power ultrafast pulse generation.[48–50] A 5 mm long Tm : Lu_2O_3 ceramic is pumped by a home-made continuous-wave

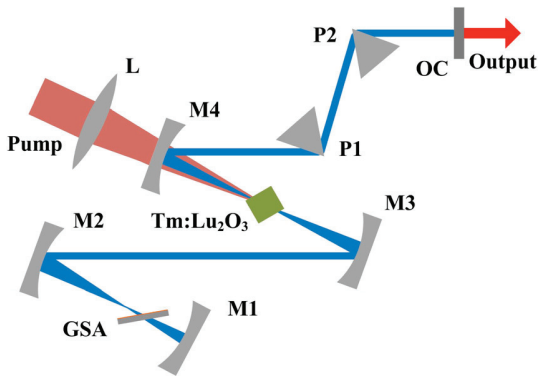

FIG. 3. Laser setup. L: lens; M1 with 75 mm curvature; M2–M4 with 100 mm curvature radii; P1, P2: fused silica prisms.

Ti:sapphire laser at 796 nm with 2.6 W maximum power. A *p*-polarized pump beam is focused into the gain medium via an 80 mm focal length lens and a folding mirror (with >99% transmittance at 976 nm) to a spot radius of 26 μm ($1/e^2$ intensity), as measured in air at the location of the input facet of the ceramic. The GSA is inserted in the cavity between mirrors M1 and M2 at the Brewster's angle, to reduce Fresnel's reflection losses (Fig. 3). The laser beam waist radii inside the gain medium and on the GSA are calculated as $32 \times 61\ \mu m^2$ and $110 \times 158\ \mu m^2$, respectively, by using the ray matrices method of Ref. 51. A pair of infrared-grade fused silica prisms with 12 cm tip-to-tip separation is used to control the intracavity net group velocity dispersion (GVD). Each prism is placed at a minimum deviation to reduce insertion losses. The total round-trip cavity GVD at 2 μm is $\sim -2980\ fs^2$, due to the insertion of the prisms (glass material dispersion, $-113\ fs^2/mm$), the gain medium itself ($-15\ fs^2/mm$) and the angular dispersion of the prism pair ($-1436\ fs^2$). The whole cavity length is ~1.35 m.

During continuous wave operation (without GSA), the laser produces up to 640 mW output power from 1.8 W of absorbed pump power at ~2070 nm, the lasing threshold being 89 mW. After inserting the GSA, the lasing threshold increases to 314 mW. Self-starting mode-locking is achieved at 160 mW average output power (with ~1.16 W absorbed pump power). The maximum average output power is 270 mW, while the absorbed pump power is 1.8 W. The obtained output power is comparable to that of previous 2 μm SESAMs mode-locked ultrafast solid-state lasers (e.g., 155 mW from Tm, Ho:NaY $(WO_4)_2$,[8] 325 mW from $Tm : Sc_2O_3$ (Ref. 9)), but larger than thus far reported for 2 μm nanotube mode-locked

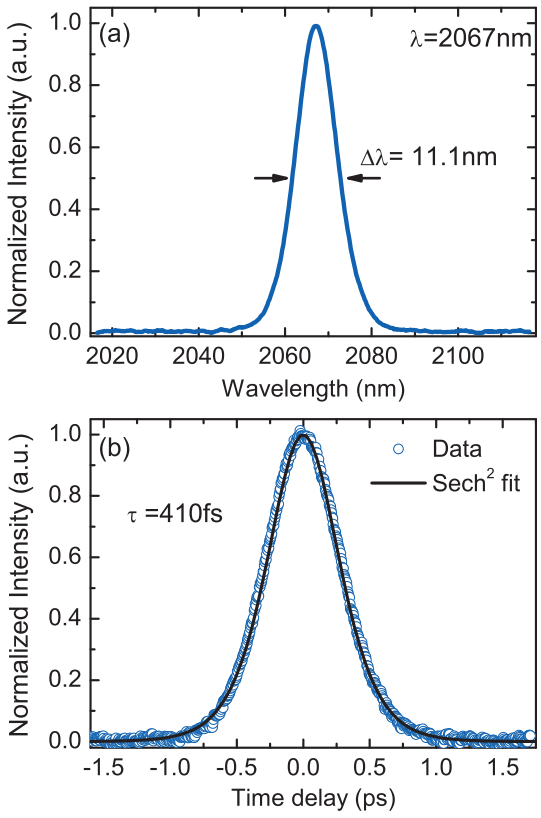

FIG. 4. (a) Output spectrum, (b) autocorrelation trace.

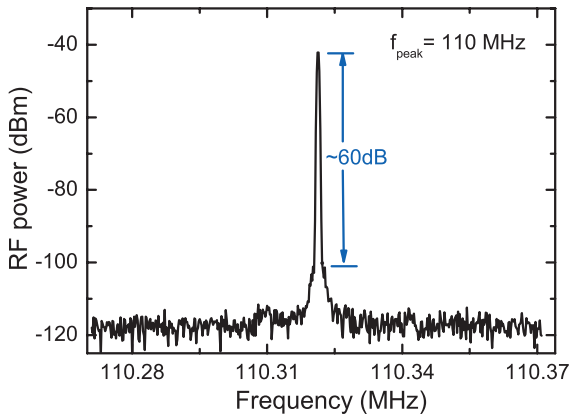

FIG. 5. RF spectrum. The resolution bandwidth is 300 Hz.

Tm-doped solid-state lasers (e.g., 50 mW from a $Tm : Lu_2O_3$ laser[52]) and graphene mode-locked solid-state lasers (e.g., 60 mW from a Tm:CLNGG laser[28]) in sub-ps regime. The repetition rate is ~110 MHz. The corresponding pulse energy is ~2.45 nJ, higher than thus far achieved for 2 μm nanotube (e.g., ~0.5 nJ (Refs. 53–55)) and graphene (e.g., ~0.4 nJ (Ref. 25)) mode-locked fiber lasers. Higher output power/energy is possible by increasing pump power, as the output power is limited by the maximum available pump power.

The mode-locked pulse peak wavelength is 2067 nm (Fig. 4(a)). The FWHM bandwidth is ~11.1 nm at the maximum average output power. The spectrum has no soliton sidebands, unlike what typical for 2 μm ultrafast fiber lasers[53–55] due to intracavity periodical perturbations.[56] Fig. 4(b) plots the autocorrelation trace of the output pulses at the maximum average output power. The data are well fitted by a $sech^2$ temporal profile, giving a pulse duration ~410 fs. This is longer than previously reported for SESAM and nanotube mode-locked 2 μm solid-state lasers (e.g., ~200 fs (Refs. 8, 9, and 52)), but shorter than previous graphene mode-locked 2 μm solid-state lasers (e.g., ~10 ps (Ref. 27), ~729 fs (Ref. 28)). The pulse duration is much shorter than 2 μm nanotube (e.g., ~0.75 ps) (Ref. 53), ~1.3 ps (Ref. 55)) and graphene (e.g., ~3.6 ps (Ref. 25)) mode-locked fiber lasers. The time-bandwidth product is 0.319, close to 0.315 expected for transform-limited $sech^2$ pulses.

The mode-locking operation stability is studied measuring the radio frequency (RF) spectrum using a fast InGaAs photo-detector (EOT, ET-5010; >7 GHz cut-off) connected to a spectrum analyzer. Fig. 5 plots the RF spectrum around the fundamental repetition frequency of 110 MHz. A signal-to-noise ratio of 60 dB (i.e. a contrast of 10^6) is measured, implying no Q-switching instabilities.[57]

In conclusion, we demonstrated a graphene mode-locked solid-state $Tm : Lu_2O_3$ laser at 2 μm, having transform-limited 410 fs pulses with ~270 mW average output power and ~110 MHz repetition rate. This showcases the potential of graphene for high-power ultrafast solid-state lasers.

We acknowledge funding from the ERC grant NANOPOTS, EU grants RODIN, MEM4WIN, GENIUS, EPSRC grants EP/GO30480/1 and EP/G042357/1, King's College

Cambridge, the Royal Academy of Engineering, a Royal Society Wolfson Research Merit Award, and the Cambridge Nokia Research Centre.

[1]V. W. S. Chan, IEEE J. Sel. Top. Quantum Electron. **6**, 959 (2000).
[2]B. E. Bouma, L. E. Nelson, G. J. Tearney, D. J. Jones, M. E. Brezinski, and J. G. Fujimoto, J. Biomed. Opt. **3**, 76 (1998).
[3]F. Dausinger, F. Lichtner, and H. Lubatschowski, *Femtosecond Technology for Technical and Medical Applications* (Springer, 2004).
[4]R. R. Gattass and E. Mazur, Nat. Photonics **2**, 219 (2008).
[5]M. Ebrahim-Zadeh and I. T. Sorokina, *Mid-infrared Coherent Sources and Applications* (Springer, 2008).
[6]U. Keller, Nature **424**, 831 (2003).
[7]W. Sibbett, A. A. Lagatsky, and C. T. A. Brown, Opt. Express **20**, 6989 (2012).
[8]A. A. Lagatsky, X. Han, M. D. Serrano, C. Cascales, C. Zaldo, S. Calvez, M. D. Dawson, J. A. Gupta, C. T. A. Brown, and W. Sibbett, Opt. Lett. **35**, 3027 (2010).
[9]A. A. Lagatsky, P. Koopmann, P. Fuhrberg, G. Huber, C. T. A. Brown, and W. Sibbett, Opt. Lett. **37**, 437 (2012).
[10]T. Hasan, Z. Sun, F. Wang, F. Bonaccorso, P. H. Tan, A. G. Rozhin, and A. C. Ferrari, Adv. Mater. **21**, 3874 (2009).
[11]Z. Sun, T. Hasan, and A. C. Ferrari, Physica E **44**, 1082 (2012).
[12]F. Bonaccorso, Z. Sun, T. Hasan, and A. C. Ferrari, Nat. Photonics **4**, 611 (2010).
[13]D. Popa, Z. Sun, T. Hasan, W. B. Cho, F. Wang, F. Torrisi, and A. C. Ferrari, Appl. Phys. Lett. **101**, 153107 (2012).
[14]Z. Sun, T. Hasan, F. Torrisi, D. Popa, F. Bonaccorso, D. M. Basko, and A. C. Ferrari, ACS Nano **4**, 803 (2010).
[15]F. Torrisi, T. Hasan, W. Wu, S. Jung, F. Bonaccorso, P. J. Paul, D. P. Chu, and A. C. Ferrari, ACS Nano **6**, 2992 (2012).
[16]F. Wang, A. G. Rozhin, V. Scardaci, Z. Sun, F. Hennrich, I. H. White, W. I. Milne, and A. C. Ferrari, Nat. Nanotechnol. **3**, 738 (2008).
[17]I. H. Baek, H. W. Lee, S. Bae, B. H. Hong, Y. H. Ahn, D. I. Yeom, and F. Rotermund, Appl. Phys. Express **5**, 032701 (2012).
[18]W. D. Tan, C. Y. Su, R. J. Knize, G. Q. Xie, L. J. Li, and D. Y. Tang, Appl. Phys. Lett. **96**, 031106 (2010).
[19]W. B. Cho, J. H. Yim, S. Y. Choi, S. Lee, U. Griebner, V. Petrov, and F. Rotermund, Opt. Lett. **33**, 2449 (2008).
[20]Z. Sun, D. Popa, T. Hasan, F. Torrisi, F. Wang, E. Kelleher, V. Nicolosi, and A. Ferrari, Nano Res. **3**, 653 (2010).
[21]Q. Bao, H. Zhang, Y. Wang, Z. Ni, Y. Yan, Z. X. Shen, K. P. Loh, and D. Y. Tang, Adv. Funct. Mater. **19**, 3077 (2009).
[22]T. Hasan, F. Torrisi, Z. Sun, D. Popa, V. Nicolosi, and A. C. Ferrari, Phys. Status Solidi B **247**, 2953 (2010).
[23]D. Popa, Z. Sun, F. Torrisi, T. Hasan, F. Wang, and A. C. Ferrari, Appl. Phys. Lett. **97**, 203106 (2010).
[24]Y. Hernandez, V. Nicolosi, M. Lotya, F. M. Blighe, Z. Y. Sun, S. De, I. T. McGovern, B. Holland, M. Byrne, Y. K. Gunko, J. J. Boland, P. Niraj, G. Duesberg, S. Krishnamurthy, R. Goodhue, J. Hutchison, V. Scardaci, A. C. Ferrari, and J. N. Coleman, Nat. Nanotechnol. **3**, 563 (2008).
[25]M. Zhang, E. J. R. Kelleher, F. Torrisi, Z. Sun, T. Hasan, D. Popa, F. Wang, A. C. Ferrari, S. V. Popov, and J. R. Taylor, Opt. Express **20**, 25077 (2012).
[26]L. E. Nelson, D. J. Jones, K. Tamura, H. A. Haus, and E. P. Ippen, Appl. Phys. B **65**, 277 (1997).
[27]J. Liu, Y. G. Wang, Z. S. Qu, L. H. Zheng, L. B. Su, and J. Xu, Laser Phys. Lett. **9**, 15 (2012).
[28]J. Ma, G. Q. Xie, P. Lv, W. L. Gao, P. Yuan, L. J. Qian, H. H. Yu, H. J. Zhang, J. Y. Wang, and D. Y. Tang, Opt. Lett. **37**, 2085 (2012).
[29]S. Stankovich, D. A. Dikin, G. H. B. Dommett, K. M. Kohlhaas, E. J. Zimney, E. A. Stach, R. D. Piner, S. T. Nguyen, and R. S. Ruoff, Nature **442**, 282 (2006).
[30]C. Mattevi, G. Eda, S. Agnoli, S. Miller, K. A. Mkhoyan, O. Celik, D. Mostrogiovanni, G. Granozzi, E. Garfunkel, and M. Chhowalla, Adv. Funct. Mater. **19**, 2577 (2009).
[31]S. Bae, H. Kim, Y. Lee, X. Xu, J. S. Park, Y. Zheng, J. Balakrishnan, T. Lei, H. R. Kim, Y. I. Song, Y. J. Kim, K. S. Kim, B. Ozyilmaz, J. H. Ahn, B. H. Hong, and S. Iijima, Nat. Nanotechnol. **5**, 574 (2010).
[32]F. Bonaccorso, A. Lombardo, T. Hasan, Z. Sun, L. Colombo, and A. C. Ferrari, Materials Today **15**, 14 (2012).
[33]A. C. Ferrari, J. C. Meyer, V. Scardaci, C. Casiraghi, M. Lazzeri, F. Mauri, S. Piscanec, D. Jiang, K. S. Novoselov, S. Roth, and A. K. Geim, Phys. Rev. Lett. **97**, 187401 (2006).
[34]L. G. Cancado, A. Jorio, E. H. M. Ferreira, F. Stavale, C. A. Achete, R. B. Capaz, M. V. O. Moutinho, A. Lombardo, T. S. Kulmala, and A. C. Ferrari, Nano Lett. **11**, 3190 (2011).
[35]A. Mooradian, Phys. Rev. Lett. **22**, 185 (1969).
[36]A. C. Ferrari and J. Robertson, Phys. Rev. B **61**, 14095 (2000).
[37]A. Pirkle, J. Chan, A. Venugopal, D. Hinojos, C. W. Magnuson, S. McDonnell, L. Colombo, E. M. Vogel, R. S. Ruoff, and R. M. Wallace, Appl. Phys. Lett. **99**, 122108 (2011).
[38]A. Ferrari, Solid State Commun. **143**, 47 (2007).
[39]A. Das, S. Pisana, B. Chakraborty, S. Piscanec, S. K. Saha, U. V. Waghmare, K. S. Novoselov, H. R. Krishnamurthy, A. K. Geim, A. C. Ferrari, and A. K. Sood, Nat. Nanotechnol. **3**, 210 (2008).
[40]C. Casiraghi, S. Pisana, K. S. Novoselov, A. K. Geim, and A. C. Ferrari, Appl. Phys. Lett. **91**, 233108 (2007).
[41]S. Pisana, M. Lazzeri, C. Casiraghi, K. S. Novoselov, A. K. Geim, A. C. Ferrari, and F. Mauri, Nature Mater. **6**, 198 (2007).
[42]Y. Y. Wang, Z. H. Ni, T. Yu, Z. X. Shen, Y. H. Wu, W. Chen, and A. T. Shen Wee, J. Phys. Chem. C **112**, 10637 (2008).
[43]L. Kong, J. Phys. Chem. C **114**, 21618 (2010).
[44]V. G. Kravets, A. N. Grigorenko, R. R. Nair, P. Blake, S. Anissimova, K. S. Novoselov, and A. K. Geim, Phys. Rev. B **81**, 155413 (2010).
[45]G. P. Agrawal, *Applications of Nonlinear Fiber Optics* (Academic, London, 2001).
[46]R. R. Nair, P. Blake, K. S. Novoselov, T. J. Booth, T. Stauber, N. M. R. Peres, and A. K. Geim, Science **320**, 1308 (2008).
[47]K. F. Mak, M. Y. Sfeir, Y. Wu, C. H. Lui, J. A. Misewich, and T. F. Heinz, Phys. Rev. Lett. **101**, 196405 (2008).
[48]P. Koopmann, R. Peters, K. Petermann, and G. Huber, Appl. Phys. B **102**, 19 (2011).
[49]O. L. Antipov, S. Y. Golovkin, O. N. Gorshkov, N. G. Zakharov, M. V. Kruglova, M. O. Marychev, A. A. Novikov, N. V. Sakharov, and E. V. Chuprunov, Quantum Electron. **41**, 863 (2011).
[50]A. A. Lagatsky, O. L. Antipov, and W. Sibbett, Opt. Express **20**, 19349 (2012).
[51]W. Koechner, *Solid-State Laser Engineering* (Springer, 2006).
[52]A. Schmidt, P. Koopmann, G. Huber, P. Fuhrberg, S. Y. Choi, F. Rotermund, V. Petrov, and U. Griebner, Opt. Express **20**, 5313 (2012).
[53]K. Kieu and F. W. Wise, IEEE Photon Technol. Lett. **21**, 128 (2009).
[54]S. Kivisto, T. Hakulinen, A. Kaskela, B. Aitchison, D. P. Brown, A. G. Nasibulin, E. I. Kauppinen, and O. G. Okhotnikov, Opt. Express **17**, 2358 (2009).
[55]M. A. Solodyankin, E. D. Obraztsova, A. S. Lobach, A. I. Chernov, V. I. Konov, and E. M. Dianov, Opt. Lett. **33**, 1336 (2008).
[56]M. L. Dennis and I. N. Duling, IEEE J. Quantum Electron **30**, 1469 (1994).
[57]C. Honninger, R. Paschotta, F. Morier-Genoud, M. Moser, and U. Keller, J. Opt. Soc. Am. B **16**, 46 (1999).